Studies of Electron Field Emission Processes from Low Work Function Cu-Li Edge Emitters via Photoelectron and Field Electron Emission Microscopy

R. P. Winarski,[1] J. W. Freeland,[1] J. C. Tucek,[2] O. Auciello,[2]
D. M. Gruen,[2] N. Moldovan,[1] D. C. Mancini,[1] A. P. J. Stampfl[3]

[1] *Experimental Facilities Division, Argonne National Laboratory, Argonne, IL, U.S.A.*
[2] *Materials Science Division, Argonne National Laboratory, Argonne, IL, U.S.A.*
[3] *Physics Division, Australian Nuclear Science and Technology Organisation, Lucas Heights, Australia*

Introduction

Electron field emitter arrays (FEAs) are being investigated for applications in numerous vacuum microelectronic devices.[1-10] FEAs are intense electron sources that are used in field emitter displays (FEDs), high-frequency devices, and other vacuum microelectronic applications. Improved performance has been achieved through the use of emission-enhancing coatings, including Cu-Li alloys,[3,12] that reduce the voltage required to obtain adequate stable electron emission levels. Reduced operating voltages reduce the power consumption and cost of driving electronics and increase the lifetime of these devices.

Field electron emission from a metal is due to the tunneling of electrons through the surface (solid-vacuum interface) potential barrier in the presence of an external electric field. For a typical metal, fields on the order of 10^3 V/μm are necessary to generate appreciable emission. Ways to increase the total emission current at a given electric field include increasing the local field enhancement factor through the use of geometrically sharp emitters, increasing the active emitting area (edge emitters), and lowering the work function of the emitting surface.

It has been shown that thin layers of alkali metals on metal surfaces lower the work function of the surface, producing a minimum in the effective work function for thicknesses between 0.5 and 1 monolayer of alkali atoms.[13,14] However, these coatings, a few Å thick, are physically and chemically unstable and are difficult to fabricate and maintain in such a thin, contamination-free, alkali metal layer. It has been shown that Cu-Li alloys form a stable Li monolayer on the surface that is replenished via Gibbsian segregation and bulk diffusion processes.[15,16] Cu-Li alloys have been used to fabricate edge-emitting structures with turn-on fields as low as 5 V/μm.[3] These structures combine a low work function coating, a small radius of curvature at the emission edge, and an extended emission area.

Experiment

In brief, the metal films are deposited using magnetron sputtering onto the sides of arrays of Si cylinders, with a Ta layer deposited first as a barrier to keep the Cu from diffusing into the Si. The arrays are then ion milled, and the Si core and Ta barrier are selectively etched to a depth of 5.0 μm leaving a thin metal coating on the outside of the cylinder forming the emission edge. A scanning electron microscope image of a single emitter is shown in Fig. 1.

Photoemission electron microscopy (PEEM)/field emission electron microscopy (FEEM) measurements were conducted in a UHV PEEM end station at beamline 4-ID-C, an intermediate x-ray beamline at Argonne National Laboratory's Advanced Photon Source. The beamline consists of a circular polarizing undulator and a spherical-grating monochromator, which were used to provide intense soft x-rays at the silicon K (1839 eV), and copper $L_{II,III}$ (952.3 and 932.5 eV) absorption edges. Because of the low effective work function (1.52 eV) of the Cu-20 at.% Li alloy samples, it was possible to observe significant field emission at low applied fields. By blocking the x-rays, images due solely to the field-emitted electrons were also obtained. The lateral resolution was on the order of 0.1 μm. Exposure durations of about three seconds were needed for the x-ray photoemission images and of about five minutes for the weaker field emission measurements.

Pre-absorption edge, absorption edge, and post-absorption edge images were collected around the Si K, and Cu $L_{II,III}$ absorption energies. Emission sites were identified by comparison of the corresponding x-ray photoemission electron microscopy (XPEEM) and FEEM images.
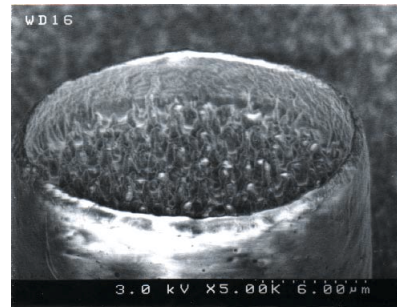
FIG. 1. *Scanning electron microscope image of a single vertical Cu-Li edge emitter.*

Results and Discussion

The present results were obtained for an array of cylindrical Cu-Li vertical edge emitters with a diameter of 100 μm on a 400 μm pitch. The emitting edge was a 500-Å-thick Cu-20 at.% Li film. These emitters have a 5 V/μm threshold, which is a factor of 4 reduction compared to arrays fabricated from 500 Å of pure Cu. An effective work function for the alloy has been determined to be 1.52 eV.[3] XPEEM could not be performed at the Li absorption edge of 54.7 eV, as this energy lies below the energy range covered by the beamline.

Shown in Fig. 2 is the Si-enhanced XPEEM image for a portion of the edge of an emitter. The figure was produced in the following manner: Two images of the same area of the emitter were acquired, one just above the Si K-edge at 1841_eV, and the other just below at 1835 eV. In order to remove the effects of background, the latter (below-edge image) was subtracted from the
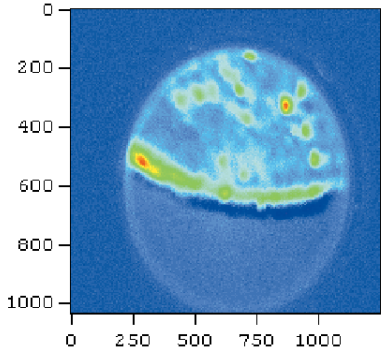
FIG. 2. *Si-enhanced XPEEM image of the edge of an emitter. The PEEM is aligned perpendicular to the surface of the substrate. Bright areas correspond to enhanced areas of Si adsorption relative to the other elements.*
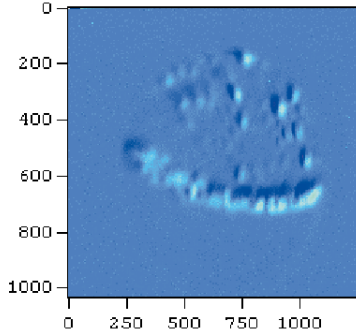
FIG. 3. *Cu-enhanced XPEEM image of the edge of an emitter. The bright outer edge corresponds to enhanced Cu adsorption relative to the other elements.*
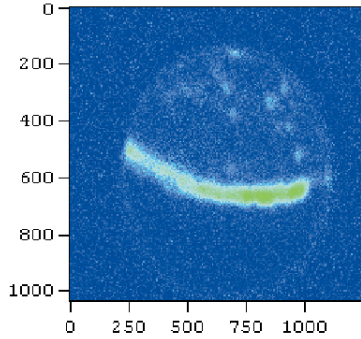
FIG. 4. *FEEM image of the emitter edge. The most intense emission occurs at the outer edge of the emitter structure corresponding to the location of the Cu-Li alloy as observed in Fig. 3.*

former (above-edge image). Si absorption is enhanced in the area inside the edge of the structure, and a smaller Si signal is observed on the extreme outside of the emitter structure. The corresponding Cu-enhanced image of the same section of the emitter is shown in Fig. 3. The maximum in the Cu absorption appears at the extreme outside edge of the structure, which is the location of the free-standing ring of Cu-Li at the edge of the Si cylinder. The location of the largest Cu signal corresponds to the decreased Si signal observed in Fig. 2.

The field emission image of the emitting edge region is obtained by blocking the x-rays and is shown in Fig. 4. The location of the most intense field emission corresponds to the location of the maximum in the Cu signal shown in Fig. 3 and, thus, corresponds to the edge of the freestanding Cu-Li cylinder itself. To a lesser extent, some emission occurs from isolated spots in the area inside the edge, corresponding to topographical features (as
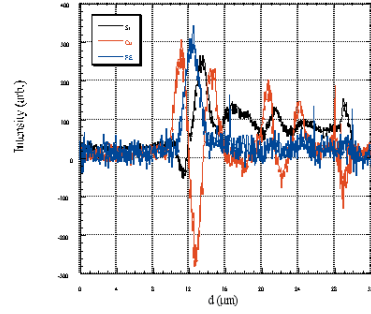
FIG. 5. *Cuts across the Si and Cu enhanced images and the field emission image in Figs. 2, 3, and 4 respectively. The peak intensity of the field emission is observed to lie between the Si and Cu signal peaks.*
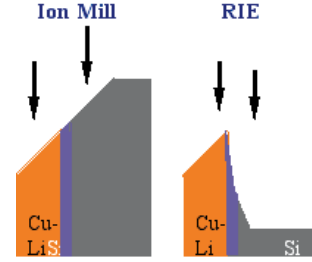
FIG. 6. *Schematic of the processing that produces the Cu-Li emission edge. After conformal thin-film deposition, normal-incidence ion milling erodes the outside edge faster than the bulk material due to the higher sputtering rate on the angled surface. Subsequent reactive ion etching removes the Si and the Ta leaving a sharp inner edge on the Cu Li film. The largest field enhancement occurs at this edge leading to increased field emission.*

seen in Fig. 2) that are a result of the Si etching process. Emission from these spots is most likely due to local field enhancement at sharp Si spikes that are formed during the reactive ion etching process, as in Fig. 1. Most importantly, the intense field emission is fairly uniform and continuous and occurs along the low work function Cu-Li edge.

To examine the features of the XPEEM images and the field emission image more closely, cuts across the emission edge were taken at the same position in order to compare the relative signal intensities of the Cu, Si, and the field emission directly. Arbitrarily normalized Cu, Si, and field emission line scans are shown in Fig. 5. As seen in Figs. 3 and 4, where the Cu signal is enhanced, the Si signal is diminished and vice versa. It is important to note that the maximum in the field emission signal occurs precisely at the Cu-Li and Si interface. This location corresponds to the sharpest portion of the Cu-Li edge, resulting from the ion milling and etching processes used to form the emitters. A schematic illustrating the formation of the edge feature is shown in Fig. 6. During the ion milling process, the outer edge of the structure is eroded at a faster rate than the material along the Si core. After etching the Si, the sharp edge on the inner side of the thin-walled hollow cylinder is exposed and hence becomes the field emission edge. The Ta layer is located between the Si and the Cu-Li, but emission is not expected to originate from the Ta because: (1) the Ta also is etched by the CF_4 that is used to etch the Si; (2) Ta is a high work function surface; and (3) Li is not soluble in Ta and, hence, no Li surface layer is expected to form on the Ta surface. Thus, the enhanced emission at the Cu-Li edge is a result of the low work function Cu-Li surface, and the electric field is locally enhanced along the inner part of the edge itself, leading to the most intense emission observed in this region.

2

Summary

Thin-film vertical electron edge-emitting structures with stable, low work function, Cu-20 at.% Li coatings have threshold fields of ~5 V/µm for field emission. These emitters have been investigated using elementally selective XPEEM and FEEM to gain insights into the nature of the emission at the edge. Emission originating at the low work function Cu-Li edge structure has been identified with XPEEM. The coupling of elementally selective XPEEM and FEEM provides an efficient means for identifying emission sites and correlating them to specific elemental layers.

Acknowledgments

References

[1] H.P. Kuo, S.F. Burriesci, J. Lin, and D.J. Miller, J. Vac. Sci. Technol. B **15**, 2782 (1997).

[2] H. Fujii, S. Kanemaru, H. Hiroshima, S.M. Gorwadkar, T. Matssukawa, and J. Itoh, Appl. Surf. Sci. **146**, 203 (1999).

[3] J.C. Tucek, A.R. Krauss, D.M. Gruen, O. Auciello, N. Moldovan, D.C. Mancini, S. Zurn, and D. Polla, J. Vac. Sci. Technol. B **18**, 2427 (2000).

[4] J.G. Fleming, D.A.A. Ohlberg, T. Felter, and M. Malinowski, J. Vac. Sci. Technol. B **14**, 1958 (1996).

[5] H.H. Busta, J. Micromech. Microeng. **7**, 37 (1997).

[6] D.S. Hsu and H.F. Gray, Thin Solid Films **286**, 92 (1996).

[7] S. Yang and M. Yokoyama, Mater. Chem. Phys. **51**, 6 (1997).

[8] K. Sawada, K. Suzuki, A.H. Jayatissa, Y. Hatanaka, and T. Ando, Jpn. J. Appl. Phys., Part 2 **36**, L965 (1997).

[9] C.G. Lee, B.G. Park, and J.D. Lee, J. Vac. Sci. Technol. B **15 464** (1997).

[10] D. Temple, Mater. Sci. Eng. **24**, 185 (1999).

[11] J.M. Macaulay, I. Brodie, C.A. Spindt, and C.E. Holland, Appl. Phys. Lett. **61**, 997 (1992).

[12] O. Auciello, A.R. Krauss, D.M. Gruen, P. Shah, T. Corrigan, M.E. Kordesch, R.P.H. Chang, and T.L. Barr, J. Appl. Phys. **85**, 8405 (1999).

[13] Z. Sidorski, I. Pelly, and R. Gomer, J. Chem. Phys. **45**, 1605 (1966).

[14] L. Schmidt and R. Gomer, J. Chem. Phys. **42**, 3573 (1965).

[15] A.R. Krauss, O. Auciello, A. Uritani, M. Valentine, M. Mendelsohn, and D.M. Gruen, Nucl. Instrum. Methods B **27**, 209 (1987).

[16] A.R. Krauss, A.B. DeWald, D.M. Gruen, and N.Q. Lam, Radiat. Eff. **89**, 129 (1985).